Hindawi Publishing Corporation
International Journal of Corrosion
Volume 2013, Article ID 139798, 13 pages
http://dx.doi.org/10.1155/2013/139798

Research Article

Adsorption Properties and Inhibition of C38 Steel Corrosion in Hydrochloric Solution by Some Indole Derivates: Temperature Effect, Activation Energies, and Thermodynamics of Adsorption

M. Lebrini, F. Robert, and C. Roos

Laboratoire Matériaux et Molécules en Milieu Amazonien, UAG-UMR ECOFOG, Campus Trou Biran, 97337 Cayenne, French Guiana

Correspondence should be addressed to C. Roos; christophe.roos@guyane.univ-ag.fr

Received 19 September 2012; Accepted 14 February 2013

Academic Editor: Vesna Mišković-Stanković

The corrosion rates in the presence of some indole derivates, namely, 9H-pyrido[3,4-b]indole (norharmane) and 1-methyl-9H-pyrido[3,4-b]indole (harmane), as inhibitors of C38 steel corrosion inhibitor in 1 M HCl solution, were measured by potentiodynamic polarization and electrochemical impedance spectroscopy (EIS) techniques, in the range of temperatures from 25 to 55°C. Results obtained revealed that the organic compounds investigated have inhibiting properties for all temperatures. The inhibition was assumed to occur via adsorption of the indole molecules on the metal surface. Adsorption of indole derivates was found to follow the Langmuir isotherm. The apparent activation energies, enthalpies, and entropies of the dissolution process and the free energies and enthalpies for the adsorption process were determined by potentiodynamic polarization and electrochemical impedance. The fundamental thermodynamic functions were used to collect important information about indole inhibitory behaviour.

1. Introduction

The effect of temperature on the inhibited acid-metal reaction is highly complex, because many changes occur on the metal surface such as rapid etching and desorption of inhibitor and the inhibitor itself may undergo decomposition and/or rearrangement. Temperature effects on acidic corrosion and corrosion inhibition of iron and steel most often in HCl and H_2SO_4 solutions had been the object of a large number of investigations [1–12]. However, it was found that few inhibitors with acid-metal systems have specific reactions which are effective (or more) at high temperature as they are at low temperature [13–15]. Thermodynamic parameters such as adsorption heat, adsorption entropy, and adsorption free energy can be obtained from experimental data of the studies of the inhibition process at different temperatures. The kinetic data such as apparent activation energy and preexponential factor at different inhibitor concentrations are calculated, and the effects of the activation energy and preexponential factor on the corrosion rate of steel were discussed [16–20].

Our earlier results obtained for 9H-pyrido[3,4-b]indole (norharmane) and 1-methyl-9H-pyrido[3,4-b]indole (harmane) as corrosion inhibitors of C38 steel demonstrated that correlation exists between the inhibition efficiency and the chemical structure [21]. It was found that these compounds are good inhibitors in acidic solutions and the inhibition efficiency of these indole-type organic compounds may be explained in terms of electronic properties (the energy of the highest occupied molecular orbital (E_{HOMO}) and the energy of the lowest unoccupied molecular orbital (E_{LUMO})). The aim of this paper is to extend these investigations in order to obtain a better understanding of the mode of inhibitory action of the harmane and norharmane by calculating thermodynamic parameters for both C38 steel dissolution and inhibitor adsorption process in hydrochloric acid solution using potentiodynamic polarization and electrochemical impedance spectroscopy (EIS).

2. Experimental

Electrode and Solution. Corrosion tests have been carried out on electrodes cut from sheets of C38 steel. Steel strips contained 0.36 wt% C, 0.66 wt% Mn, 0.27 wt% Si, 0.02 wt% S, 0.015 wt% P, 0.21 wt% Cr, 0.02 wt% Mo, 0.22 wt% Cu, 0.06 wt% Al, and the remainder iron. The specimens were embedded in epoxy resin leaving a working area of 0.78 cm^2.

Table 1: Corrosion parameters obtained from electrochemical measurements of C38 steel in 1 M HCl containing various concentrations of indole derivates at 25°C.

Inhibitor	Polarisation curves			EIS		
	E_{corr} versus SCE (mV)	I_{corr} (μA·cm^{-2})	IE (%)	R_{ct} (Ω·cm^2)	C_{dl} (μF·cm^{-2})	IE (%)
1 M HCl	−529	284	—	49 ± 0.02	546	
Norharmane						
0.2 mM	−467	67	76	148 ± 0.91	183	67
0.4 mM	−476	61	79	238 ± 1.65	120	79
0.8 mM	−494	52	82	514 ± 1.18	55	90
1.2 mM	−455	28	90	641 ± 1.73	44	92
Harmane						
0.2 mM	−476	65	77	181 ± 0.10	330	73
0.4 mM	−489	55	81	321 ± 0.97	270	85
0.8 mM	−479	34	88	537 ± 0.17	188	91
1.2 mM	−492	24	91	735 ± 0.68	148	93

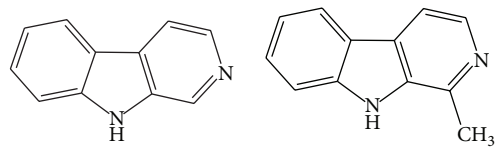

(a) (b)

Figure 1: Chemical formulas of the tested inhibitors (a) norharmane and (b) harmane.

The working surface was subsequently ground with 180 and 1200 grit grinding papers, cleaned by distilled water and ethanol. The solutions (1 M HCl) were prepared by dilution of an analytical reagent grade 33% HCl with doubly distilled water. All the tests were performed in the range of temperatures from 25 to 55°C. The tested inhibitors are 9H-pyrido[3,4-b]indole (norharmane) and 1-methyl-9H-pyrido[3,4-b]indole (harmane); their molecular structures are shown in Figure 1. The investigated compounds were commercial products: norharmane (Aldrich, P99%), harmane (Sigma, P98%), the concentration range of inhibitor employed was 0.2 mM M to 1.2 mM. The concentration of inhibitor was determined in accordance with its solubility. Varela et al. reports the solubility of norharmane and harmane in water at 20°C, at pH 7 and 13, using the absorbance at the maxima in the absorption spectra of saturated solutions [22]. The solubility of norharmane was 1.86 mM (pH = 7) and 1.81 mM (pH = 13). For harmane, the solubility was 1.61 mM (pH = 7) and 0.786 mM (pH = 13). At lower pH (Our experimental conditions, pH = 0), where the cationic form is the predominant species, all the compounds present a very high solubility, and it was not possible to obtain data with this technique at lower pH.

Electrochemical Measurements. Electrochemical measurements, including potentiodynamic polarization curves and electrochemical impedance spectroscopy (EIS), were performed in a three-electrode cell. C38 steel specimen was used as the working electrode, a platinum wire as the counter, and a saturated calomel electrode (SCE) as the reference. Before potentiodynamic test and EIS experiments, the electrode was allowed to corrode freely and its open circuit potential (OCP) was recorded as a function of time during 3 h, the time necessary to reach a quasi-stationary value for the open-circuit potential. This steady-state OCP corresponds to the corrosion potential (E_{corr}) of the working electrode. The anodic and cathodic polarisation curves were recorded by a constant sweep rate of 20 mV min^{-1}. Electrochemical impedance spectroscopy (EIS) measurements were carried out, using ac signals of amplitude 5 mV peak to peak in the frequency range of 100 kHz to 10 mHz. Electrochemical measurements were performed through a VSP electrochemical measurement system (Bio-Logic). The above procedures were repeated two times with success for each concentration of the two tested inhibitors. The Tafel fit and EIS data were analysed using graphing and analyzing impedance software, version EC-Lab V9.97.

3. Results and Discussion

3.1. Effect of Concentration. The corrosion rates of metals and alloys in aggressive solutions can be determined using different electrochemical methods. Electrochemical impedance spectroscopy and polarisation curves were thus employed in the present work to study the effect of indole derivates concentration. The percentages of inhibition efficiency and values of associated electrochemical parameters are listed in Table 1. Inspections of the obtained data reveal that the I_{corr} values decrease considerably in the presence of harmane and norharmane with increasing inhibitor concentration. The E_{corr} values shifted to more positive potentials in the presence of indole derivates concentration, although there was not

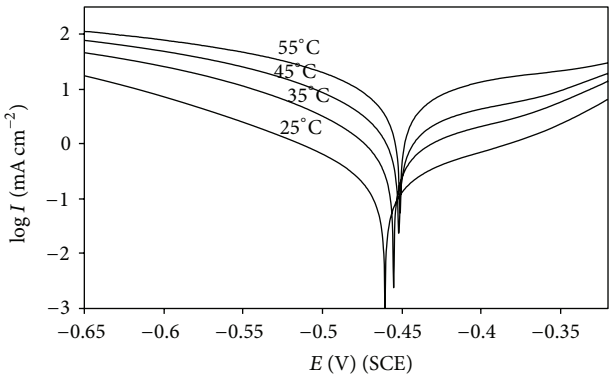

Figure 2: Effect of temperature on the cathodic and anodic responses for C38 steel in 1 M HCl.

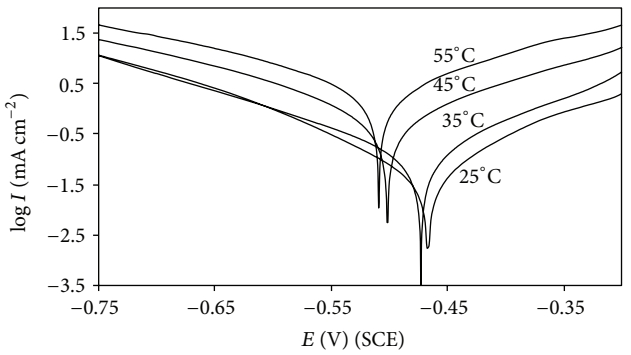

Figure 3: Effect of temperature on the cathodic and anodic responses for C38 steel in 1 M HCl + 0.2 mM of norharmane.

a specific relation between E_{corr} and inhibitors concentration. This effect may be related to the adsorption of the organic compound at the active sites of the electrode surface, retarding the corrosion reaction. The data also reveal that the addition of harmane or norharmane causes a significant increase in R_{ct} in the additive-free solution and diminishes the value of C_{dl}. The decrease in C_{dl} could be attributed to the adsorption of the inhibitors forming a protective layer on the metal surface [23]. The inhibition efficiencies, calculated from ac impedance study, show the same trend as these obtained from polarization measurements. However, IE (%) increases with inhibitor concentrations for both inhibitors, reaching a maximum value at 1.2 mM. It was found that these compounds are good inhibitors in acidic solutions and the inhibition efficiency of these indole-type organic compounds may be explained in terms of electronic properties. The detailed study of 1 M HCl at 25°C is reported in [21].

3.2. Effect of Temperature

3.2.1. Potentiodynamic Polarisation. In order to get more information about the performance of indole derivates, the nature of adsorption isotherm, and thereafter to evaluate the adsorption and activation processes, the influence of temperature is studied by potentiodynamic polarisation. Some of the polarisation curves for C38 steel electrode in 1 M HCl in

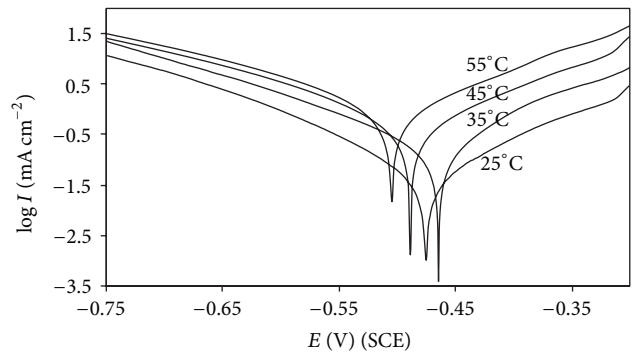

Figure 4: Effect of temperature on the cathodic and anodic responses for C38 steel in 1 M HCl + 0.2 mM of harmane.

the absence and in the presence of 0.2 mM of norharmane and harmane in the temperature range 25–55°C are given in Figures 2, 3, and 4, respectively. As it can be seen, raising the temperature increases both anodic and cathodic reactions of C38 steel electrode both in the absence and in the presence of inhibitors. Polarisation curves of the C38 steel electrode in 1 M HCl without and with addition of various concentrations of harmane at 45°C are shown in Figure 5, representative example. As it can be seen, the anodic and cathodic reactions are affected by the addition of inhibitor. Similar observations were found for all concentrations studied in the presence of both inhibitors. Accurate evaluation of Tafel slopes by Tafel extrapolation is often impossible, simply because an experimental polarization curve does not exhibit linear Tafel regions [24–27]. Our experimental polarization curves presented here do not display the expected log/linear Tafel behaviour with anodic branches exhibiting curvature over the complete applied potential range. The curvature of the anodic branch may be attributed to the deposition of the corrosion products or impurities in the steel (e.g., Fe_3C) to form a nonpassive surface film [24]. The various electrochemical parameters were calculated from Tafel plots and summarized in Table 2. The inhibition efficiency and the surface coverage degree (θ) values for steel are also shown in the same table. The surface coverage θ was calculated from (1) [28]. It has been observed from Table 2, that the corrosion current density (I_{corr}) increased with increasing temperature in both uninhibited and inhibited solutions. The addition of norharmane or harmane to the HCl solution shifts the E_{corr} towards more negative values at all of the studied temperatures, although there was not a specific relation between E_{corr} and inhibitors concentration. The IE (%) values decrease with increasing temperature; a decrease in inhibition efficiencies with the increase in temperature might be due to weakening of physical adsorption. Consider

$$\theta = \frac{I_{corr} - I_{corr(inh)}}{I_{corr}}, \quad (1)$$

where I_{corr} and $I_{corr(inh)}$ are the corrosion current density values in the absence and presence of indole derivates, respectively.

Table 2: Electrochemical parameters calculated from Tafel plots and the corresponding inhibition efficiencies at various temperatures studied of C38 steel in 1 M HCl containing different concentrations of indole derivates.

		Norharmane						Harmane					
Temp. (°C)	Con. (mM)	E_{corr} versus SCE (mV)	I_{corr} (μA·cm^{-2})	b_a (mV·dec^{-1})	b_c (mV·dec^{-1})	IE (%)	θ	E_{corr} versus SCE (mV)	I_{corr} (μA·cm^{-2})	b_a (mV·dec^{-1})	b_c (mV·dec^{-1})	IE (%)	θ
25	1 M HCl	−460	232	106	89	—	—	—	—	—	—	—	—
	0.2	−467	67	107	125	76	0.7641	−476	65	110	124	77	0.7711
	0.4	−476	61	116	122	79	0.7852	−489	55	98	107	81	0.8063
	0.8	−494	52	97	118	82	0.8169	−479	34	113	119	88	0.8803
	1.2	−455	28	93	112	90	0.9014	−492	24	87	107	91	0.9155
35	1 M HCl	−454	843	111	109	—	—	—	—	—	—	—	—
	0.2	−473	236	112	144	72	0.7200	−465	212	118	133	75	0.7485
	0.4	−472	195	109	126	77	0.7687	−470	182	116	136	78	0.7841
	0.8	−470	165	102	131	80	0.8043	−456	154	109	128	82	0.8173
	1.2	−479	98	103	135	88	0.8837	−464	101	103	118	88	0.8802
45	1 M HCl	−451	1192	120	109	—	—	—	—	—	—	—	—
	0.2	−501	512	130	146	57	0.5705	−496	413	117	134	65	0.6535
	0.4	−509	472	112	115	60	0.6040	−488	389	112	125	67	0.6737
	0.8	−505	443	135	135	63	0.6284	−487	335	113	126	72	0.7190
	1.2	−485	352	107	140	70	0.7047	−484	245	110	118	79	0.7945
55	1 M HCl	−450	1982	131	116	—	—	—	—	—	—	—	—
	0.2	−509	1023	142	150	48	0.4839	−504	983	136	148	50	0.5040
	0.4	−497	954	114	156	52	0.5187	−496	852	123	140	57	0.5701
	0.8	−566	867	117	127	56	0.5626	−564	715	110	146	64	0.6393
	1.2	−494	651	109	139	67	0.6715	−515	574	107	132	71	0.7104

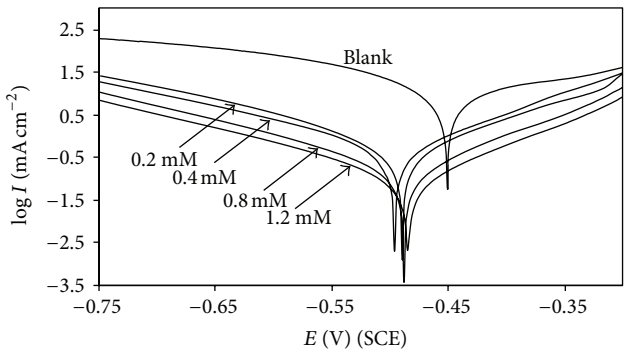

Figure 5: Polarisation curves for C38 steel in 1 M HCl containing different concentrations of harmane at 45°C.

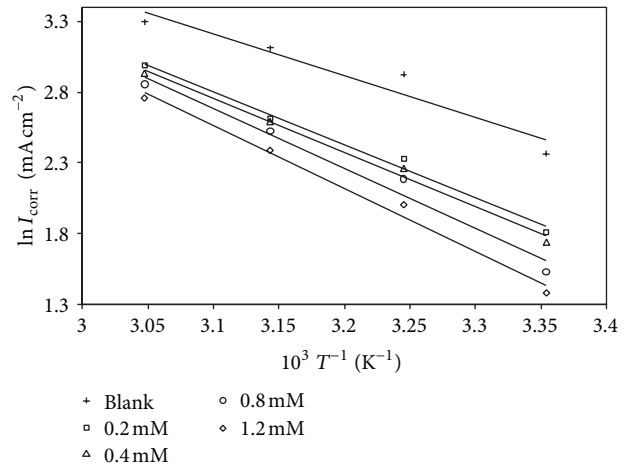

Figure 6: Arrhenius plots of corrosion $\ln(I_{corr})$ versus $1/T$ of 1 M HCl and at different concentrations of harmane.

In order to calculate activation parameters for the corrosion process, Arrhenius (2) and an alternative formulation of Arrhenius (3) were used:

$$I_{corr} = K \exp\left(\frac{-E_a}{RT}\right), \quad (2)$$

$$I_{corr} = \frac{RT}{Nh} \exp\left(\frac{\Delta S_a}{R}\right) \exp\left(-\frac{\Delta H_a}{RT}\right), \quad (3)$$

where I_{corr} is the corrosion current density, K the Arrhenius preexponential constant, E_a is the activation energy for the corrosion process, h is the Plank's constant, N is the Avogadro's number, the enthalpy of activation (ΔH_a), and the entropy of activation (ΔS_a).

Arrhenius plots for the corrosion density of C38 steel in the case of harmane are given in Figure 6, representative example. Similar plots are obtained in the case of norharmane. The apparent activation energies (E_a) at different concentrations of indole derivates were determined by linear regression between $\ln I_{corr}$ and $1/T$ and the result is shown in Table 3. All the linear regression coefficients were close to 1, indicating that the C38 steel corrosion in hydrochloric acid can be elucidated using the kinetic model. Inspection of Table 3 showed that the values of E_a determined in 1 M HCl

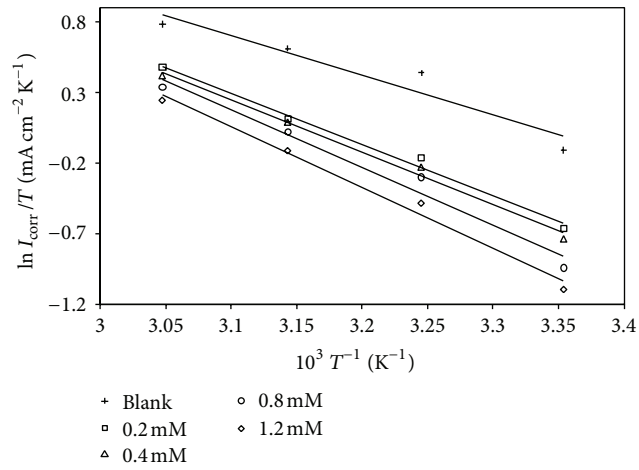

Figure 7: Arrhenius plots of corrosion $\ln(I_{corr}/T)$ versus $1/T$ of 1 M HCl and at different concentrations of harmane.

containing indole derivates are higher than that for uninhibited solution. The increase in the apparent activation energy may be interpreted as physical adsorption that occurs in the first stage [29]. Moreover, the values obtained for norharmane are somewhat higher than those obtained for harmane and confirm the fact that the inhibitor efficiency of norharmane is slightly lower than that of harmane. Szauer and Brand explained that the increase in activation energy can be attributed to an appreciable decrease in the adsorption of the inhibitor on the steel surface with increase in temperature [30]. Figure 7 showed a plot of $\ln(I_{corr}/T)$ versus $1/T$ with a slope of $(-\Delta H_a/R)$ and an intercept $(\ln R/Nh + \Delta S_a/R)$ from which the values of ΔH_a and ΔS_a were calculated, respectively. All estimated kinetic-thermodynamic parameters were tabulated also in Table 3. Inspection of these data revealed that the thermodynamic parameters (ΔH_a and ΔS_a) for dissolution reaction of C38 steel in 1 M HCl in the presence of both inhibitors are higher than that of in the absence of inhibitors. The positive signs of ΔH_a reflect the endothermic nature of the steel dissolution process suggesting that the dissolution of steel is slow in the presence of inhibitors [31]. Furthermore, the values obtained for norharmane are somewhat higher than those obtained for harmane and confirm the fact that the inhibitor efficiency of norharmane is slightly lower than that of harmane. One can notice that E_a and ΔH_a values vary in the same way for both inhibitors (Table 3). The values of ΔS_a were negative both in the absence and presence of inhibitors, implying that the activated complex represented the rate-determining step with respect to the association rather than the dissociation step. It means that a decrease in disorder occurred when proceeding from the reactants to the activated complex [30]. Also, the ΔS_a shift can be explained as a result of the replacement process of water molecules during adsorption of organic inhibitor on the steel surface.

3.2.2. Impedance Measurements. The corrosion behaviour of C38 steel in 1 M HCl solution in the presence of indole derivates was also investigated by EIS in the temperature range 25–55°C. The EIS of C38 steel electrode in 1 M HCl

Table 3: Thermodynamic parameters calculated from Tafel plots for the adsorption of indole derivates in 1 M HCl on the C38 steel at different temperatures.

Con. (mM)	Norharmane			Harmane		
	E_a (kJ mol^{-1})	ΔH_a (kJ mol^{-1})	ΔS_a (J mol^{-1} K^{-1})	E_a (kJ mol^{-1})	ΔH_a (kJ mol^{-1})	ΔS_a (J mol^{-1} K^{-1})
HCl	24.42	23.29	−119.48	—	—	—
0.2	31.73	30.60	−99.81	31.20	30.07	−101.88
0.4	32.38	31.25	−98.12	31.80	30.67	−100.43
0.8	33.40	32.27	−95.27	35.18	34.05	−90.53
1.2	37.99	36.85	−81.97	36.89	35.76	−86.63

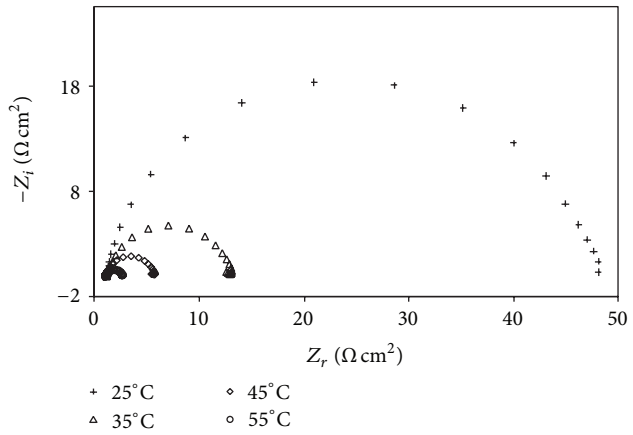

Figure 8: Nyquist diagrams for C38 steel in 1 M HCl at different temperatures.

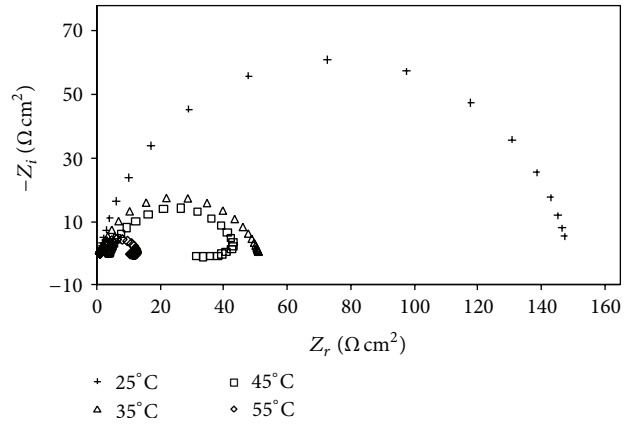

Figure 9: Nyquist diagrams for C38 steel in 1 M HCl containing 0.2 mM of norharmane at different temperatures.

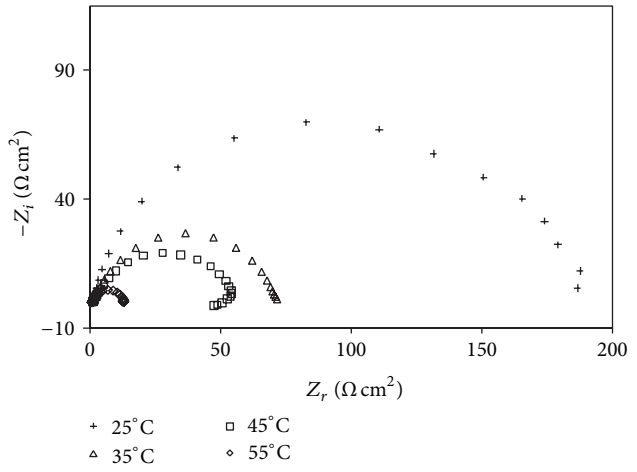

Figure 10: Nyquist diagrams for C38 steel in 1 M HCl containing 0.2 mM of harmane at different temperatures.

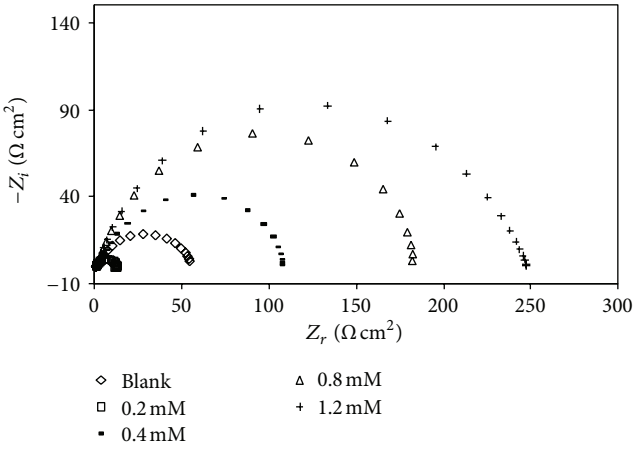

Figure 11: Nyquist diagrams for C38 steel in 1 M HCl containing different concentrations of noharmane at 35°C.

solution in the absence and in the presence of of 0.2 mM of noharmane and harmane, at different temperatures, are shown in Figures 8, 9, and 10; representative example. Figure 11 shows the impedance plots of C38 steel electrode in 1 M HCl solution in the absence and presence of different concentrations of norharmane at 35°C. It can be seen that, the size of the capacitive loop increased by increasing the concentration of norharmane. All the impedance spectra were measured at the corresponding open-circuit potentials. After analyzing the shape of the Nyquist plots, it is concluded that the curves obtained up to 45°C approximated by a single capacitive semi-circles, showing that the corrosion process was mainly charge transfer controlled. The general shape of the curves is very similar for all concentrations studied. The diameter of Nyquist plots (R_{ct}) decreases with increasing temperature for both inhibitors. For the most temperatures 45 and 55°C, an inductive loop appeared at low-frequency

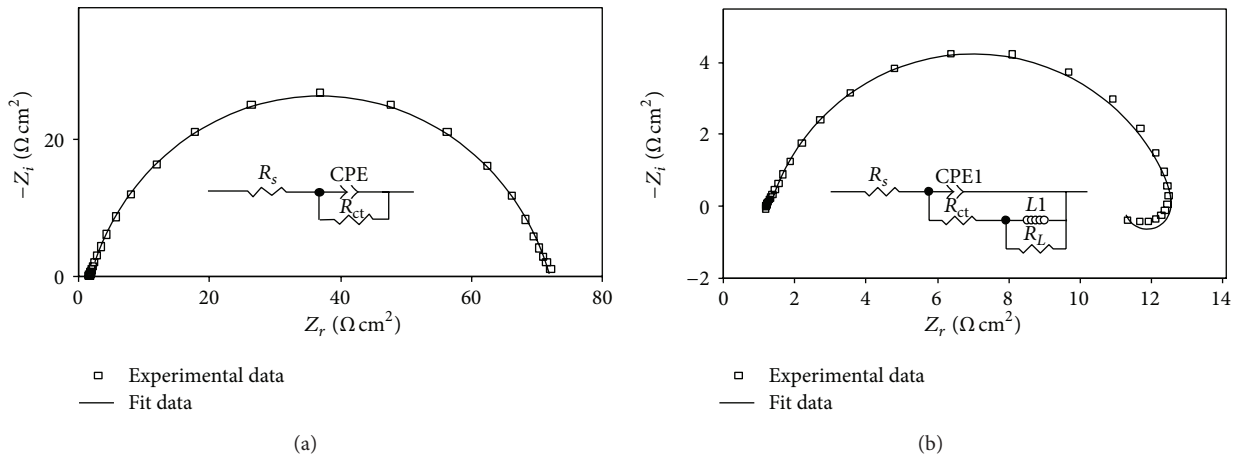

Figure 12: Nyquist plots: (□) experimental data and (—) fit data, together with the equivalent circuit used to fit the impedance data, recorded for a C38 electrode (a) in 1 M HCl solution + 0.2 mM harmane at 35°C and (b) in 1 M HCl solution + 0.2 mM norharmane at 55°C.

values. Similar observations were found for all concentrations studied. The presence of the LF inductive loop may be attributed to the relaxation process obtained by adsorption species like Cl^-_{ads} and H^+_{ads} on the electrode surface [32–35]. It may also be attributed to the adsorption of inhibitor on the electrode surface [36] or to the redissolution of the passivated surface at low frequencies [37]. The above impedance diagrams (Nyquist) contain depressed semicircles with the center under the real axis; such behaviors characteristic for solid electrodes and often referred to as frequency dispersion have been attributed to roughness and inhomogeneities of the solid surfaces, impurities [38–41]. Therefore, a constant phase element (CPE) instead of a capacitive element is used to get a more accurate fit of experimental data set. For analysis of the impedance spectra exhibiting one capacitive loop, the equivalent circuit (EC) given in Figure 12(a) was used to fit the experimental spectra while the EC shown in Figure 12(b) was used for the impedance spectra containing one capacitive loop and an inductive loop. Simulation of Nyquist plots with above models shows excellent agreement with experimental data (Figures 12(a) and 12(b); representative example).

The parameters calculated with the application of these models are summarized in Tables 4 and 5. The values discussed show that the organic compounds investigated have inhibiting properties for all temperature values. This conclusion is based on the values of R_{ct} in inhibitors presence. They are greater than those in 1 M HCl. The temperature rise leads to a decrease of R_{ct} values. This is due, on one hand, to the increase of the rate of metal dissolution and, on the other hand, to the shift of the adsorption/desorption equilibrium towards the inhibitor's desorption and hence to the decrease of surface coverage degree. The n value almost decreases with temperature increase and this is interpreted as an evidence for surface inhomogeneity increase. The latter is attributed to the accelerated corrosion and the developed metal surface. At lower temperatures the inhibitors adsorb on the most active surface sites; this results in a decrease of surface inhomogeneity. The desorption, which is favored by high temperatures, will increase with this effect. The C_{dl} value was calculated using (4) [42–44]:

$$C_{dl} = \left(A \cdot {R_{ct}}^{1-n}\right)^{1/n}. \quad (4)$$

It is clear that the addition of harmane or norharmane causes a significant increase in C_{dl} in the additive-free solution for all temperatures studied. As the double layer capacitance can be connected with the thickness of the layer of adsorbed inhibitor molecules at the interface and this dependence is of reverse proportionality; it follows that the thickness of the adsorption layer will decrease with temperature increase. Similar tendency was found for CPE constant (A) for all temperatures studied. It can be seen from Tables 2, 4, and 5 that the inhibition efficiencies calculated by both methods show the same trend. The IE (%) values decrease with increasing temperature and no difference of numerical values of inhibition efficiencies was observed at 25 and 35°C. However the results obtained at 45 and 55°C show a difference in numerical values obtained by both methods. This variation may be due to the difference between methods, which each method is realised differently with some conditions and assumptions.

To obtain the activation parameters from the impedance technique, values of R_{ct} and those of β_a and β_c obtained at different temperatures were used to calculate values of I_{corr} according to Stern-Geary [45] equation:

$$I_{corr} = \frac{\beta_a \beta_c}{2.303\left(\beta_a + \beta_c\right)}\left(\frac{1}{R_{ct}}\right). \quad (5)$$

Figures 13 and 14 show the Arrhenius plot for the results obtained in 1 M HCl solutions in the presence of harmane, representative example. Similar plots are obtained in the case of norharmane. The results are in good agreement with those obtained from polarization studies and show the same trend. The difference of numerical values of ΔS_a determined from the two techniques may be attributed to the different methods that have been used for the determination of the corrosion rates.

Table 4: Values of the elements of equivalent circuit required for fitting the EIS for C38 steel immersed in the presence and absence of norharmane at different temperatures.

	Temp (°C)	R_{ct} ($\Omega\,cm^2$)	$A10^4$ ($\Omega^{-1}\,s^n\,cm^{-2}$)	n	C_{dl} ($\mu F\,cm^{-2}$)	L ($H\,cm^{-2}$)	R_L ($\Omega\,cm^2$)	IE (%)	θ
Blank	25	49 ± 0.02	9.5 ± 0.73	0.853 ± 0.014	546	—	—	—	—
	35	17 ± 0.64	20.5 ± 4.21	0.795 ± 0.421	863	18 ± 1.87	6 ± 1.26	—	—
	45	12 ± 0.94	43.5 ± 3.56	0.745 ± 0.362	1583	15 ± 2.35	3 ± 0.87	—	—
	55	3 ± 0.96	72.8 ± 5.64	0.735 ± 0.093	1834	10 ± 8.54	2 ± 1.25	—	—
0.2 mM	25	148 ± 0.91	2.91 ± 0.02	0.871 ± 0.008	183	—	—	67	0.6689
	35	53 ± 0.43	4.37 ± 0.25	0.836 ± 0.053	209	—	—	60	0.6038
	45	30 ± 0.35	10.88 ± 3.65	0.765 ± 0.059	380	25 ± 4.61	9 ± 1.78	50	0.5000
	55	10 ± 0.65	13.35 ± 1.75	0.815 ± 0.120	501	2 ± 0.40	2 ± 1.37	50	0.5000
0.4 mM	25	238 ± 1.65	1.89 ± 0.19	0.872 ± 0.005	120	—	—	79	0.7941
	35	95 ± 0.89	3.53 ± 0.14	0.829 ± 0.052	175	—	—	78	0.7789
	45	55 ± 3.04	6.19 ± 0.94	0.790 ± 0.032	252	10 ± 1.20	15 ± 1.60	73	0.7273
	55	14 ± 0.93	8.84 ± 2.31	0.831 ± 0.054	362	3 ± 0.21	2 ± 0.32	64	0.6429
0.8 mM	25	514 ± 1.18	0.84 ± 0.03	0.883 ± 0.012	55	—	—	90	0.9047
	35	180 ± 1.04	3.18 ± 0.13	0.825 ± 0.045	173	—	—	82	0.8235
	45	85 ± 1.56	5.01 ± 0.30	0.814 ± 0.023	244	7 ± 0.27	14 ± 0.90	79	0.7857
	55	22 ± 1.55	7.13 ± 0.47	0.809 ± 0.251	267	6 ± 1.60	2 ± 1.10	77	0.7727
1.2 mM	25	641 ± 1.73	0.66 ± 0.02	0.887 ± 0.010	44	—	—	92	0.9236
	35	245 ± 0.55	2.3 ± 0.78	0.803 ± 0.072	114	—	—	91	0.9143
	45	123 ± 0.81	2.9 ± 0.57	0.802 ± 0.140	127	—	—	88	0.8780
	55	25 ± 0.41	4.46 ± 0.17	0.804 ± 0.023	149	6 ± 0.50	3 ± 1.43	80	0.8000

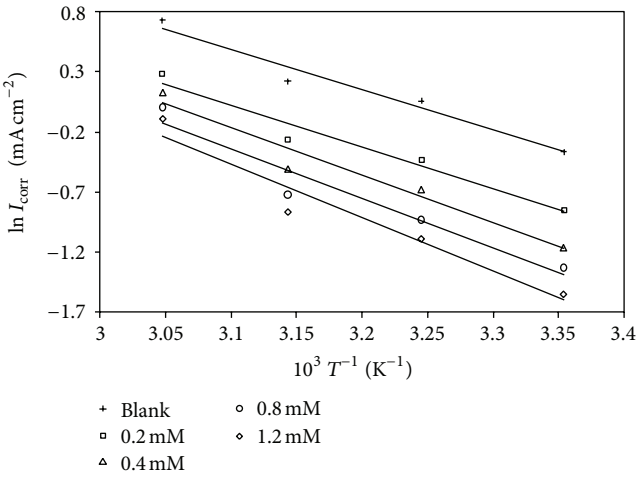

Figure 13: Arrhenius plots $\ln I_{corr}$ versus $1/T$ of 1 M HCl and at different concentrations of harmane.

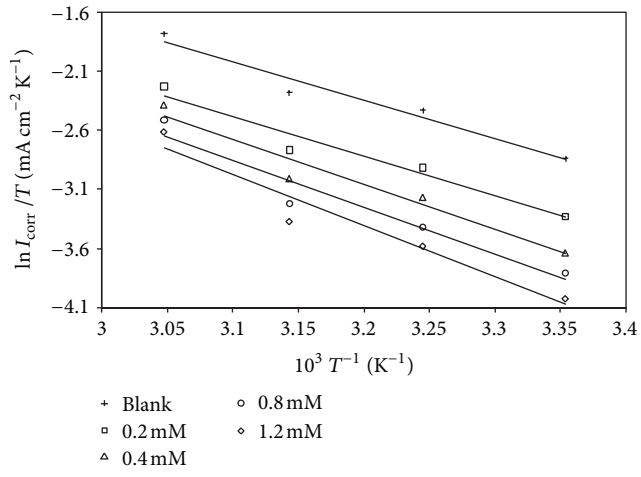

Figure 14: Arrhenius plots of corrosion $\ln(I_{corr}/T)$ versus $1/T$ of 1 M HCl at different concentrations of harmane.

3.3. Adsorption Isotherm. Inhibition by organic compounds is, mainly, due to their ability to adsorb onto a metal surface to form a protective film. The establishment of isotherms that describe the adsorption behaviour of corrosion inhibitor is important as they provide important information about the nature of metal-inhibitor interaction. It has been reported that the adsorption of the inhibitor molecules depends on a variety of factors such as the presence of functional groups (either electron donating or withdrawing), charge distribution at the donor atom, the π orbital character of donating electrons, the nature of substrate metal and the type of interaction between organic molecules and the metallic surface as well.

The most frequently used isotherms are Langmiur (6), Temkin (7), and Frumkin (8). All these isotherms are tested. In all cases, the degree of surface coverage (θ) is plotted as a function of the inhibitor concentration (C_{inh}). In the present study, values of θ are obtained from I_{corr} and R_{ct}. The significance of the adsorption isotherm was obtained by calculating the correlation coefficients (R^2). As an example,

Table 5: Values of the elements of equivalent circuit required for fitting the EIS for C38 steel immersed in the presence and absence of harmane at different temperatures.

	Temp (°C)	R_{ct} (Ω cm^2)	$A10^4$ (Ω^{-1} s^n cm^{-2})	n	C_{dl} (μF cm^{-2})	L (H cm^{-2})	R_L (Ω cm^2)	IE (%)	θ
Blank	25	49 ± 0.02	9.5 ± 0.73	0.853 ± 0.014	546	—	—	—	—
	35	17 ± 0.64	20.5 ± 4.21	0.795 ± 0.421	863	18 ± 1.87	6 ± 1.26	—	—
	45	12 ± 0.94	43.5 ± 3.56	0.745 ± 0.362	1583	15 ± 2.35	3 ± 0.87	—	—
	55	3 ± 0.96	72.8 ± 5.64	0.735 ± 0.093	1834	10 ± 8.54	2 ± 1.25	—	—
0.2 mM	25	181 ± 0.10	4.82 ± 0.19	0.866 ± 0.042	330	—	—	73	0.7293
	35	73 ± 0.61	6.92 ± 0.44	0.816 ± 0.501	353	—	—	71	0.7123
	45	50 ± 1.23	9.73 ± 0.27	0.805 ± 0.062	468	25 ± 8.41	8 ± 3.02	70	0.7000
	55	16 ± 0.81	19.5 ± 4.03	0.719 ± 0.501	503	11 ± 0.34	3 ± 0.8	69	0.6875
0.4 mM	25	321 ± 0.97	3.71 ± 0.37	0.870 ± 0.036	270	—	—	85	0.8474
	35	129 ± 0.65	5.29 ± 0.09	0.804 ± 0.074	275	—	—	84	0.8372
	45	82 ± 1.54	7.95 ± 1.02	0.784 ± 0.128	375	25 ± 1.74	9 ± 1.5	82	0.8171
	55	21 ± 2.31	10.31 ± 2.13	0.824 ± 0.054	455	21 ± 0.58	4 ± 1.3	76	0.7619
0.8 mM	25	537 ± 0.17	2.52 ± 0.27	0.873 ± 0.051	188	—	—	91	0.9088
	35	218 ± 0.56	3.96 ± 0.72	0.795 ± 0.104	211	—	—	90	0.9037
	45	136 ± 1.53	4.37 ± 0.73	0.811 ± 0.091	226	—	—	89	0.8897
	55	27 ± 1.20	8.64 ± 2.03	0.780 ± 0.035	299	5 ± 0.12	2 ± 0.76	81	0.8148
1.2 mM	25	735 ± 0.68	1.92 ± 0.12	0.883 ± 0.036	148	—	—	93	0.9333
	35	293 ± 0.54	3.28 ± 0.27	0.814 ± 0.037	192	—	—	93	0.9283
	45	182 ± 0.53	4.33 ± 0.07	0.826 ± 0.051	254	—	—	92	0.9176
	55	32 ± 0.66	7.36 ± 1.91	0.783 ± 0.102	260	11 ± 1.54	5 ± 0.8	84	0.8438

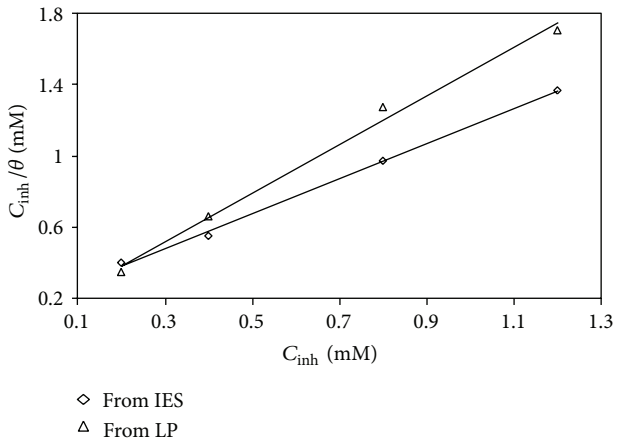

Figure 15: Langmuir adsorption plots for C38 steel in 1 M HCl containing different concentrations of norharmane at 55°C.

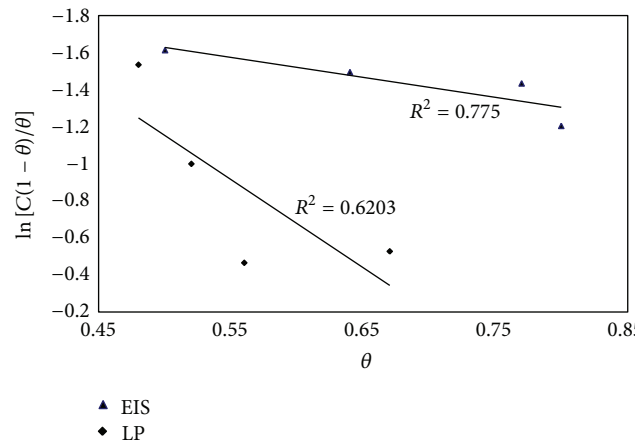

Figure 16: Frumkin adsorption plots for C38 steel in 1 M HCl containing different concentrations of norharmane at 55°C.

Figures 15, 16, and 17 represent fitting of impedance and polarization data obtained for C38 electrode in 1 M HCl containing various concentrations of norharmane at 55°C to Langmuir, Temkin, and Frunkin isotherms. The best correlation between the experimental results, obtained from the three tested isotherm functions, was obtained using Langmuir isotherm (the strong correlation $R^2 = 0.999$ for both methods). Similar observations were found for all temperatures studied. The simplest, being the Langmuir isotherm, is based on assumption that all adsorption sites are equivalent and that particle binding occurs independently from nearby sites being occupied or not [46]. Consider

$$\frac{C_{inh}}{\theta} = \frac{1}{K} + C_{inh} \quad \text{(Langmuir isotherm)}, \tag{6}$$

$$\left(\frac{\theta}{1-\theta}\right)\exp(-2a\theta) = KC_{inh} \quad \text{(Frumkin isotherm)}, \tag{7}$$

$$\exp(-2a\theta) = KC_{inh} \quad \text{(Temkin isotherm)}, \tag{8}$$

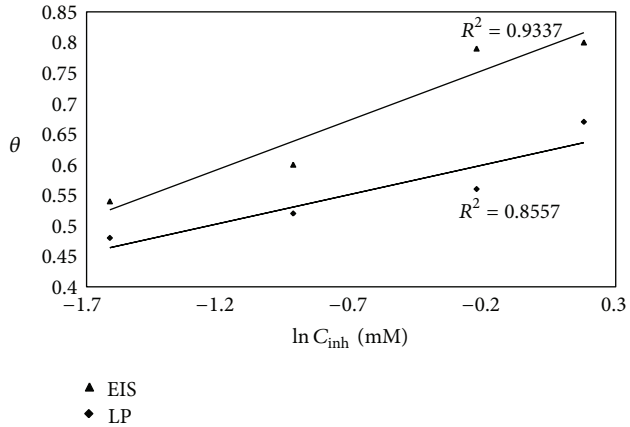

Figure 17: Temkin adsorption plots for C38 steel in 1 M HCl containing different concentrations of norharmane at 55°C.

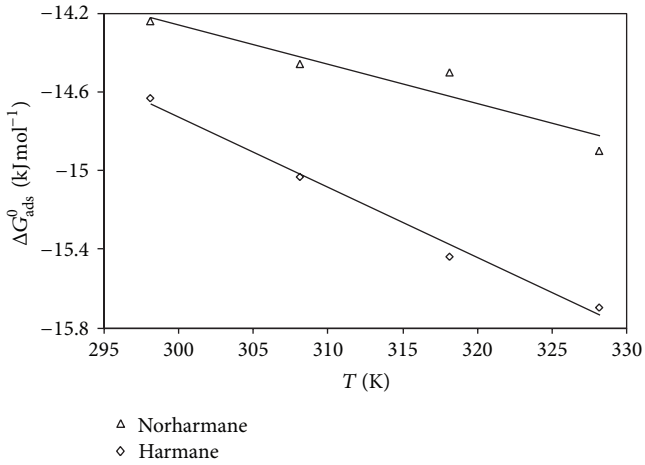

Figure 18: Variation of ΔG^0_{ads}, evaluated from IES, versus T on C38 steel in 1 M HCl containing indole derivates.

where "K" is the binding constant of the adsorption reaction and "a" is the lateral interaction term describing the molecular interactions in the adsorption layer and the heterogeneity of the surface.

The well known thermodynamic adsorption parameters are the standard free energy of adsorption (ΔG^0_{ads}), the heat of adsorption (ΔH^0_{ads}), and the standard entropy of adsorption (ΔS^0_{ads}). These quantities can be calculated depending on the estimated values of K from adsorption isotherms at different temperatures.

The constant of adsorption, K, is related to the standard free energy of adsorption, ΔG^0_{ads}, with the following equation:

$$K = \frac{1}{55.5} \exp\left(\frac{-\Delta G^0_{ads}}{RT}\right). \quad (9)$$

The value 55.5 in the above equation is the concentration of water in solution in mol L^{-1} [47]. The ΔG^0_{ads} values at all studied temperatures can be calculated. Then, the obtained ΔG^0_{ads} values plotted versus T (Figures 18 and 19) gave the heat

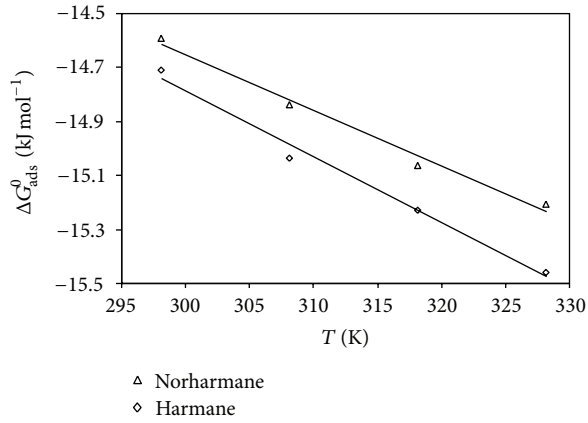

Figure 19: Variation of ΔG^0_{ads}, evaluated from LP, versus T on C38 steel in 1 M HCl containing indole derivates.

of adsorption ΔH^0_{ads} and the standard adsorption entropy ΔS^0_{ads} in accordance with the basic equation:

$$\Delta G^0_{ads} = \Delta H^0_{ads} - T\Delta S^0_{ads}. \quad (10)$$

All thermodynamic adsorption parameters estimated from both methods for indole derivates on C38 steel from 1 M of HCl solution are listed in Tables 6, 7, and 8. The entire values of thermodynamic adsorption obtained by both methods are in good agreement and follow the same trend. The negative values of ΔG^0_{ads} ensure the spontaneity of the adsorption process and stability of the adsorbed layer on the steel surface. The calculated ΔG^0_{ads} values indicate the physical nature of adsorption of norharmane and harmane. The dependence of ΔG^0_{ads} on experimental temperature can be summarized in two cases as follows.

(a) Value of ΔG^0_{ads} becomes less negative with increasing temperature indicating the occurrence of exothermic process at which adsorption was unfavourable with increasing reaction temperature as the result of the inhibitor desorption from the steel surface [48].

(b) Value of ΔG^0_{ads} becomes more negative with increasing temperature indicating the occurrence of endothermic process at which increasing temperature facilitates inhibitor adsorption.

The first case (a) is observed for the adsorption of the studied inhibitor species on C38 steel surface from HCl solution depending on the applied temperature range (Tables 7 and 8), indicating the occurrence of exothermic adsorption processes. Also, it is noteworthy feature that the calculated value of ΔG^0_{ads} at 25°C in the case of harmane is greater than that in the case of norharmane, which means that the electrostatic interaction between the harmane and the steel surface is stronger. This is in good agreement with the range of the inhibition efficiency values obtained at 25°C from both impedance and polarisation measurements. However in the temperature range 35–55°C, there is an observable contradiction between the results of inhibition efficiency values and the finding of the calculated value of ΔG^0_{ads}. The negative sign of (ΔH^0_{ads}) reveals that the adsorption of inhibitor molecules is

Table 6: Thermodynamic parameters calculated from IES for the adsorption of indole derivates in 1 M HCl on the C38 steel at different temperatures.

Con. (mM)	Norharmane			Harmane		
	E_a (kJ mol^{-1})	ΔH_a (kJ mol^{-1})	ΔS_a (J mol^{-1} K^{-1})	E_a (kJ mol^{-1})	ΔH_a (kJ mol^{-1})	ΔS_a (J mol^{-1} K^{-1})
HCl	28.00	26.87	−131.04	—	—	—
0.2	32.78	31.65	−120.35	29.03	27.91	−131.68
0.4	33.34	32.22	−116.44	32.82	31.69	−121.55
0.8	38.00	36.87	−105.77	34.05	32.92	−119.20
1.2	38.77	37.64	−104.36	37.05	35.92	−110.91

Table 7: Thermodynamic parameters calculated from IES for the adsorption of indole derivates on C38 steel in 1 M HCl at different temperatures.

Temp. (°C)	Norharmane			Harmane		
	ΔG^0_{ads} (kJ mol^{-1})	ΔH^0_{ads} (kJ mol^{-1})	ΔS^0_{ads} (J mol^{-1} K^{-1})	ΔG^0_{ads} (kJ mol^{-1})	ΔH^0_{ads} (kJ mol^{-1})	ΔS^0_{ads} (J mol^{-1} K^{-1})
25	−18.00			−14.63		
35	−14.46	−8.18	20.2	−15.03	−3.94	36
45	−14.50			−15.44		
55	−14.90			−15.69		

Table 8: Thermodynamic parameters calculated from LP for the adsorption of indole derivates on C38 steel in 1 M HCl at different temperatures.

Temp. (°C)	Norharmane			Harmane		
	ΔG^0_{ads} (kJ mol^{-1})	ΔH^0_{ads} (kJ mol^{-1})	ΔS^0_{ads} (J mol^{-1} K^{-1})	ΔG^0_{ads} (kJ mol^{-1})	ΔH^0_{ads} (kJ mol^{-1})	ΔS^0_{ads} (J mol^{-1} K^{-1})
25	−14.59			−14.71		
35	−14.84	−8.45	20.7	−15.04	−7.43	24.5
45	−15.06			−15.23		
55	−15.21			−15.46		

an exothermic process. Generally, an exothermic adsorption process suggests either physisorption or chemisorption while endothermic process is attributed to chemisorption [17]. Moreover, the values obtained for harmane are somewhat higher than those obtained for norharmane. This result indicated that harmane is more strongly adsorbed on the steel surface. This is in good agreement with the results obtained from impedance and polarisation measurements. The results show a great difference between the value of ΔH^0_{ads} for harmane obtained from EIS (−3.88 kJ mol^{-1}) and from LP (−7.40 kJ mol^{-1}). This difference may be due to the accuracy of linear regression between ΔG^0_{ads} and T, where the linear regression coefficient (R^2) obtained from EIS is 0.9905 and from LP is 0.9254. The ΔS^0_{ads} values in the presence of indole derivates are large and positive, meaning that an increasing in disordering takes place in going from reactants to the metal-adsorbed species reaction complex [49].

The integrated version of the Van't Hoff equation expressed by (11) can be also deduced the ΔH^0_{ads} value [50]:

$$\ln K = -\frac{\Delta H^0_{ads}}{RT} + \text{constant}. \quad (11)$$

Figures 20 and 21 show the plot of $\ln K$ versus $1/T$ from both methods which gives straight lines with slopes of $(-\Delta H^0_{ads}/R)$ and intercepts of $(-\Delta S^0_{ads}/R + \ln 1/55.5)$. The

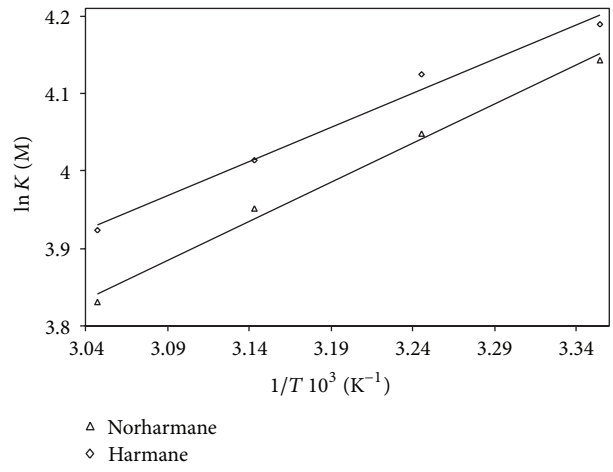

Figure 20: Van't Hoff plots for the C38 steel/indoles/1 M HCl system evaluated from LP.

calculated ΔH^0_{ads} using the Van't Hoff equation are −8.25 (from IES) and −8.41 (from LP) kJ mol^{-1} for norharmane. For harmane, the calculated ΔH^0_{ads} are −3.88 (from IES) and −7.40 (from LP) kJ mol^{-1}. These results confirm the exothermic behaviour of the adsorption of the inhibitors on the steel surface, therefore, the physisorption process. Values of

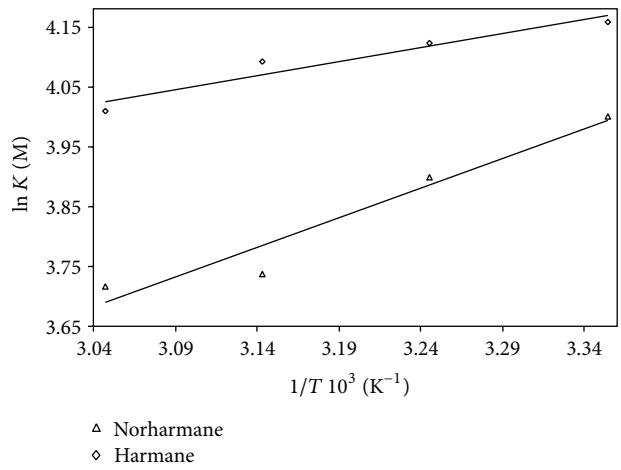

Figure 21: Van't Hoff plots for the C38 steel/indoles/1 M HCl system evaluated from IES.

ΔH^0_{ads} obtained by both (9) and (10) are in good agreement. Moreover, the deduced ΔS^0_{ads} values ($-20.01\,J\,mol^{-1}\,K^{-1}$ from IES and $-20.82\,J\,mol^{-1}\,K^{-1}$ from LP) and ($-36.14\,J\,mol^{-1}\,K^{-1}$ from IES and $-24.63\,J\,mol^{-1}\,K^{-1}$ from LP) for norharmane and harmane, respectively, are very close to those obtained in Tables 7 and 8.

4. Conclusion

Norharmane and harmane were found to be inhibitors for C38 steel corrosion in 1 M HCl solution and their inhibition efficiency increased with increasing concentration. Indole derivates are found to affect both the anodic and cathodic processes and their inhibition efficiencies decrease with increasing temperature. Impedance measurements show that the interface studied (in presence of the compounds investigated) is described by a relatively simple structural model, which shows the presence of one time constant and dispersed capacitance. For the most temperatures 45 and 55°C, an inductive loop appeared at low-frequency values. The structural parameters calculated show decrease of the resistance R_{ct} and increase of the capacitance. The inhibition is attributed to physisorption of the heterocyclic compound on the steel surface and blocking its active sites. The activation parameters of corrosion process such as activation energy, E_a, activation enthalpy, ΔH_a, and activation entropy, ΔS_a, were calculated from the dependence of corrosion rates on the temperature from polarization and impedance measurements. Also, the thermodynamic adsorption parameters were calculated and commented on from polarization and impedance measurements. The adsorption of indole derivates on the mild steel surface in 1 M HCl obeyed the Langmuir adsorption isotherm model at all studied temperatures.

References

[1] A. Khamis, M. M. Saleh, and M. I. Awad, "Synergistic inhibitor effect of cetylpyridinium chloride and other halides on the corrosion of mild steel in 0.5 M H_2SO_4," *Corrosion Science*, vol. 66, pp. 343–349, 2013.

[2] R. Sharmila, N. Selvakumar, and K. Jeyasubramanian, "Evaluation of corrosion inhibition in mild steel using cerium oxide nanoparticles," *Materials Letters*, vol. 91, pp. 78–80, 2013.

[3] L. Fragoza-Mar, O. Olivares-Xometl, M. A. Domínguez-Aguilar, E. A. Flores, P. Arellanes-Lozada, and F. Jiménez-Cruz, "Corrosion inhibitor activity of 1,3-diketone malonates for mild steel in aqueous hydrochloric acid solution," *Corrosion Science*, vol. 61, pp. 171–184, 2012.

[4] G. Quartarone, L. Ronchin, A. Vavasori, C. Tortato, and L. Bonaldo, "Inhibitive action of gramine towards corrosion of mild steel in deaerated 1.0 M hydrochloric acid solutions," *Corrosion Science*, vol. 64, pp. 82–89, 2012.

[5] M. K. Pavithra, T. V. Venkatesha, M. K. Punith Kumar, and H. C. Tondan, "Inhibition of mild steel corrosion by Rabeprazole sulfide," *Corrosion Science*, vol. 60, pp. 104–111, 2012.

[6] S. E. Nataraja, T. V. Venkatesha, K. Manjunatha, B. Poojary, M. K. Pavithra, and H. C. Tandon, "Inhibition of the corrosion of steel in hydrochloric acid solution by some organic molecules containing the methylthiophenyl moiety," *Corrosion Science*, vol. 53, no. 8, pp. 2651–2659, 2011.

[7] M. A. Hegazy, H. M. Ahmed, and A. S. El-Tabei, "Investigation of the inhibitive effect of p-substituted 4-(N,N,N-dimethyldodecylammonium bromide)benzylidene-benzene-2-yl-amine on corrosion of carbon steel pipelines in acidic medium," *Corrosion Science*, vol. 53, no. 2, pp. 671–678, 2011.

[8] M. M. Solomon, S. A. Umoren, I. I. Udosoro, and A. P. Udoh, "Inhibitive and adsorption behaviour of carboxymethyl cellulose on mild steel corrosion in sulphuric acid solution," *Corrosion Science*, vol. 52, no. 4, pp. 1317–1325, 2010.

[9] I. Ahamad and M. A. Quraishi, "Mebendazole: new and efficient corrosion inhibitor for mild steel in acid medium," *Corrosion Science*, vol. 52, no. 2, pp. 651–656, 2010.

[10] A. Popova, E. Sokolova, S. Raicheva, and M. Christov, "AC and DC study of the temperature effect on mild steel corrosion in acid media in the presence of benzimidazole derivatives," *Corrosion Science*, vol. 45, no. 1, pp. 33–58, 2003.

[11] H. L. Wang, H. B. Fan, and J. S. Zheng, "Corrosion inhibition of mild steel in hydrochloric acid solution by a mercapto-triazole compound," *Materials Chemistry and Physics*, vol. 77, no. 3, pp. 655–661, 2003.

[12] A. Popova, M. Christov, and A. Vasilev, "Inhibitive properties of quaternary ammonium bromides of N-containing heterocycles on acid mild steel corrosion—part II: EIS results," *Corrosion Science*, vol. 49, no. 8, pp. 3290–3302, 2007.

[13] M. M. Singh and A. Gupta, "Inhibition of mild steel corrosion in formic acid solution," *Bulletin of Electrochemistry*, vol. 12, no. 9, pp. 511–516, 1996.

[14] M. H. Wahdan, A. A. Hermas, and M. S. Morad, "Corrosion inhibition of carbon-steels by propargyltriphenylphosphonium bromide in H_2SO_4 solution," *Materials Chemistry and Physics*, vol. 76, no. 2, pp. 111–118, 2002.

[15] F. Bentiss, M. Lebrini, and M. Lagrenée, "Thermodynamic characterization of metal dissolution and inhibitor adsorption processes in mild steel/2,5-bis(n-thienyl)-1,3,4-thiadiazoles/hydrochloric acid system," *Corrosion Science*, vol. 47, no. 12, pp. 2915–2931, 2005.

[16] M. M. Osman, "Hexadecyl trimethyl ammonium bromide as an effective inhibitor for the corrosion of steel in sulphuric acid solution," *Anti-Corrosion Methods and Materials*, vol. 45, no. 3, pp. 176–180, 1998.

[17] W. Durnie, R. D. Marco, A. Jefferson, and B. Kinsella, "Development of a structure activity relationship for oil field corrosion

inhibitors," *Journal of the Electrochemical Society*, vol. 146, no. 5, pp. 1751–1756, 1999.

[18] L. Tang, G. Mu, and G. Liu, "The effect of neutral red on the corrosion inhibition of cold rolled steel in 1.0 M hydrochloric acid," *Corrosion Science*, vol. 45, no. 10, pp. 2251–2262, 2003.

[19] T. Zhao and G. Mu, "The adsorption and corrosion inhibition of anion surfactants on aluminium surface in hydrochloric acid," *Corrosion Science*, vol. 41, no. 10, pp. 1937–1944, 1999.

[20] M. H. Wahdan, "The synergistic inhibition effect and thermodynamic properties of 2-mercaptobenzimidazol and some selected cations as a mixed inhibitor for pickling of mild steel in acid solution," *Materials Chemistry and Physics*, vol. 49, no. 2, pp. 135–140, 1997.

[21] M. Lebrini, F. Robert, H. Vezin, and C. Roos, "Electrochemical and quantum chemical studies of some indole derivatives as corrosion inhibitors for C38 steel in molar hydrochloric acid," *Corrosion Science*, vol. 52, no. 10, pp. 3367–3376, 2010.

[22] A. P. Varela, M. D. Miguel, A. L. Maqanita, H. D. Burrows, and R. S. Becker, "Beta-carboline photosensitizers. 3. Studies on ground and excited state partitioning in AOT/water/cyclohexane microemulsions," *The Journal of Physical Chemistry*, vol. 99, no. 43, pp. 16093–16100, 1995.

[23] M. Lebrini, M. Lagrenée, H. Vezin, M. Traisnel, and F. Bentiss, "Experimental and theoretical study for corrosion inhibition of mild steel in normal hydrochloric acid solution by some new macrocyclic polyether compounds," *Corrosion Science*, vol. 49, no. 5, pp. 2254–2269, 2007.

[24] D. A. Jones, *Principles and Prevention of Corrosion*, MaCmillan, New York, NY, USA, 1992.

[25] H. J. Flitt and D. P. Schweinsberg, "A guide to polarisation curve interpretation: deconstruction of experimental curves typical of the $Fe/H_2O/H^+/O_2$ corrosion system," *Corrosion Science*, vol. 47, no. 9, pp. 2125–2156, 2005.

[26] H. J. Flitt and D. Paul Schweinsberg, "Evaluation of corrosion rate from polarisation curves not exhibiting a Tafel region," *Corrosion Science*, vol. 47, no. 12, pp. 3034–3052, 2005.

[27] F. Mansfeld, "Tafel slopes and corrosion rates obtained in the pre-Tafel region of polarization curves," *Corrosion Science*, vol. 47, no. 12, pp. 3178–3186, 2005.

[28] E. Khamis, "Effect of temperature on the acidic dissolution of steel in the presence of inhibitors," *Corrosion*, vol. 46, no. 6, pp. 476–484, 1990.

[29] S. Martinez and I. Stern, "Thermodynamic characterization of metal dissolution and inhibitor adsorption processes in the low carbon steel/mimosa tannin/sulfuric acid system," *Applied Surface Science*, vol. 199, no. 1–4, pp. 83–89, 2002.

[30] T. Szauer and A. Brand, "Mechanism of inhibition of electrode reactions at high surface coverages—II," *Electrochimica Acta*, vol. 26, no. 9, pp. 1219–1224, 1981.

[31] N. M. Guan, L. Xueming, and L. Fei, "Synergistic inhibition between *o*-phenanthroline and chloride ion on cold rolled steel corrosion in phosphoric acid," *Materials Chemistry and Physics*, vol. 86, no. 1, pp. 59–68, 2004.

[32] M. A. Amin, S. S. Abd El-Rehim, E. E. F. El-Sherbini, and R. S. Bayyomi, "The inhibition of low carbon steel corrosion in hydrochloric acid solutions by succinic acid—part I: weight loss, polarization, EIS, PZC, EDX and SEM studies," *Electrochimica Acta*, vol. 52, no. 11, pp. 3588–3600, 2007.

[33] H. J. W. Lenderrink, M. V. D. Linden, and J. H. W. De Wit, "Corrosion of aluminium in acidic and neutral solutions," *Electrochimica Acta*, vol. 38, no. 14, pp. 1989–1992, 1993.

[34] M. Kedam, O. R. Mattos, and H. Takenouti, "Reaction model for iron dissolution studied by electrode impedance I . Experimental results and reaction model," *Journal of the Electrochemical Society*, vol. 128, no. 2, pp. 257–266, 1981.

[35] M. A. Veloz and I. Gonzalez, "Electrochemical study of carbon steel corrosion in buffered acetic acid solutions with chlorides and H_2S," *Electrochimica Acta*, vol. 48, no. 2, pp. 135–144, 2002.

[36] M. S. Morad, "An electrochemical study on the inhibiting action of some organic phosphonium compounds on the corrosion of mild steel in aerated acid solutions," *Corrosion Science*, vol. 42, no. 8, pp. 1307–1326, 2000.

[37] E. M. Sherif and S. M. Park, "Effects of 1,4-naphthoquinone on aluminum corrosion in 0.50 M sodium chloride solutions," *Electrochimica Acta*, vol. 51, no. 7, pp. 1313–1321, 2006.

[38] Z. B. Stoynov, B. M. Grafov, B. Savova-Stoynova, and V. V. Elkin, *Electrochemical Impedance*, Nauka, Moscow, Russia, 1991.

[39] F. B. Growcock and R. J. Jasinski, "Time resolved impedance spectroscopy of mild steel in concentrated hydrochloric acid," *The Journal of the Electrochemical Society*, vol. 136, no. 8, pp. 2310–2314, 1989.

[40] P. Li, J. Y. Lin, K. L. Tan, and J. Y. Lee, "Electrochemical impedance and X-ray photoelectron spectroscopic studies of the inhibition of mild steel corrosion in acids by cyclohexylamine," *Electrochimica Acta*, vol. 42, no. 4, pp. 605–615, 1997.

[41] D. A. Lopez, S. N. Simison, and S. R. de Sanchez, "The influence of steel microstructure on CO_2 corrosion. EIS studies on the inhibition efficiency of benzimidazole," *Electrochimica Acta*, vol. 48, no. 7, pp. 845–854, 2003.

[42] S. Martinez and M. Metikos-Hukovic, "A nonlinear kinetic model introduced for the corrosion inhibitive properties of some organic inhibitors," *Journal of Applied Electrochemistry*, vol. 33, no. 12, pp. 1137–1142, 2003.

[43] X. Wu, H. Ma, S. Chen, Z. Xu, and A. Sui, "General equivalent circuits for Faradaic electrode processes under electrochemical reaction control," *The Journal of the Electrochemical Society*, vol. 146, no. 5, pp. 1847–1853, 1999.

[44] H. Ma, X. Cheng, G. Li et al., "The influence of hydrogen sulfide on corrosion of iron under different conditions," *Corrosion Science*, vol. 42, no. 10, pp. 1669–1683, 2000.

[45] M. Stern and A. L. Geary, "Electrochemical polarization I . A theoretical analysis of the shape of polarization curves," *The Journal of the Electrochemical Society*, vol. 104, no. 1, pp. 56–63, 1957.

[46] H. A. Sorkhabi, B. Shaabani, and D. Seifzadeh, "Effect of some pyrimidinic Shciff bases on the corrosion of mild steel in hydrochloric acid solution," *Electrochimica Acta*, vol. 50, no. 16-17, pp. 3446–3452, 2005.

[47] J. Flis and T. Zakroczymski, "Impedance study of reinforcing steel in simulated pore solution with tannin," *The Journal of the Electrochemical Society*, vol. 143, no. 8, pp. 2458–2464, 1996.

[48] L. Tang, G. Mu, and G. Liu, "The effect of neutral red on the corrosion inhibition of cold rolled steel in 1.0 M hydrochloric acid," *Corrosion Science*, vol. 45, no. 10, pp. 2251–2262, 2003.

[49] G. Banerjee and S. N. Malhotra, "Contribution to adsorption of aromatic amines on mild steel surface from HCl solutions by impedance, UV, and Raman spectroscopy," *Corrosion*, vol. 48, no. 1, pp. 10–15, 1992.

[50] D. Do, *Adsorption Analysis: Equilibria and Kinetics*, Imperial College Press, New York, NY, USA, 1998.